Knowledge-Based Systems 122 (2017) 199–213

Contents lists available at ScienceDirect

Knowledge-Based Systems

journal homepage: www.elsevier.com/locate/knosys

Linear parameter varying (LPV) based robust control of type-I diabetes driven for real patient data

Levente Kovács

Physiological Controls Research Center, University Research and Innovation Center, Óbuda University John von Neumann Faculty of Informatics, Óbuda University Bécsi út 96/b, H-1034 Budapest, Hungary

ARTICLE INFO

Article history:
Received 15 September 2016
Revised 5 February 2017
Accepted 7 February 2017
Available online 7 February 2017

Keywords:
Modern robust control
H_∞ control
LPV modeling
Nonlinearity
Type 1 diabetes

ABSTRACT

Due to increasing prevalence of diabetes as well as increasing management costs, the artificial control of diabetes is a highly important task. Model-based design allows finding more effective solutions for the individual treatment of diabetic patients, but robustness is an important property that can be hardly guaranteed by the already developed individualized control algorithms. Modern robust control (known as H_∞) theory represents an efficient possibility to solve robustness requirements in a general way based on exact mathematical formulation (Linear Matrix Inequalities) combined with knowledge-based expertise (through real patient data, uncertainty weighting functions can be formulated). When the difference between the nominal model and real patient dynamics is bounded and known, this approach becomes highly reliable. However, this requirement poses the greatest limitation since a model always represents an approximation of the complex physiological process. Consequently, the uncertainty formulation of the neglected dynamics becomes crucial as robust methods are very sensitive to them. In order to formulate them, large amount of real patient data and medical expertise is needed to cover the different life-style scenarios (especially the worst-case ones) that define the control space by the accumulated knowledge. On the other hand, H_∞–based methods represent linear control techniques; hence their direct nonlinear application is important for a physiological process. The paper presents a roadmap of using modern robust control in diabetes focusing on nonlinear model-based interpretation: how the weighting functions should be selected based on (knowledge-based) medical expertise, the direct nonlinear applicability of the method taking additional advantage of the recently emerged Linear Parameter Varying (LPV) methodology, robust performance investigation and switching control possibilities. During the control characteristics discussion, the trade-off between the medical knowledge-based empiricism and exact control engineering formulation is introduced through different examples computed under MATLAB on real diabetic patient data.

1. Introduction

1.1. Diabetes modeling and control. Artificial pancreas

Glucose is the primary source of energy of the human body. The blood glucose level is kept in a narrow range (3.9–6 mmol/L or 70–110 mg/dL) by the complex endocrine system and insulin plays a key role in this process. When insulin secretion or insulin action is impaired, diabetes is diagnosed [1].

Diabetes is named by the World Health Organization (WHO) as the “disease of the future”, predicting that the number of diabetic patients will be doubled from 2000 to 2030 [2]. Recent statistics updated the forecast for the 2010–2030 period, but still a significant increase of the overall diabetes population is predicted [3]. Consequently, the treatment of diabetes is of paramount importance. From engineering point of view, the treatment of diabetes mellitus can be represented as a control problem to automatically regulate the glucose-insulin balance. The problem is known as the Artificial Pancreas (AP) [4], investigated for type 1 diabetes mellitus (T1DM), an autoimmune type of diabetes in which the pancreatic β-cells are completely destroyed (and, as a result, the treatment requires glucose concentration measurements and subcutaneous insulin injections). The AP has three main components [5]:

- Continuous Glucose Monitors (CGM) for the subcutaneous measurement (with 5 minutes sampling time) of glucose concentration;

E-mail address: kovacs.levente@nik.uni-obuda.hu

http://dx.doi.org/10.1016/j.knosys.2017.02.008

- Insulin pumps for the subcutaneous delivery of insulin;
- Control algorithm that - based on CGM measurements - is able to determine the necessary insulin dosage to be injected by the insulin pumps.

As sophisticated CGM and insulin pumps are available on the market, the realization of an AP relies on control algorithm aspects [6–7].

The control methods proposed in the literature are mostly model-based [8]; hence, an adequate mathematical model of the human metabolism was needed. Different models appeared over the last decades, starting with the oversimplified minimal model [9]; however, nowadays more complex models are considered for describing the different compartments (at different levels of the human body), the nonlinear physiological relation of the glucose-insulin behavior, but taking the different time delays into account or including CGM models and subcutaneous insulin delivery models as well [10–12]. Although different control algorithms have been proposed in the literature [4–8], only four main control strategies reached AP prototype systems: Proportional Integral Derivative (PID) based controllers [13], Model Predictive Control (MPC) [14–17], run-to-run control [18], and Fuzzy Logic based controls [19]. The majority of the mentioned algorithms are able to achieve nocturnal glucose regulation in an individualized manner. MPC focuses on glucose trend estimations by minimizing the difference between the predicted blood glucose level estimated in a given time horizon (due to meal intakes this is usually in the 60–240 minutes interval) and the ideal glucose concentration. The PID control idea relies on continuously adjusting the insulin injection rate based on the main components of the classical control theory: proportional (based on real and ideal glucose level difference), integral (based on glucose trajectory area) and derivative (based on glucose rate change) components. The fuzzy logic based control creates a rule-based methodology. Although all the above mentioned solutions require a considerable amount of expertise converted into controller design requirements, robustness remains a challenge in all the mentioned cases that should be separately treated, discussed and implemented from the individualized control idea. Most importantly, the worst cases should be detected and handled; these can be basically translated in avoiding the hypoglycemic episodes in case of diabetic patients. This requires a large amount of measurement data not only to define the boundaries of the control space, but to supplement the model inaccuracies which are consequences of the unhandled dynamics and neglected uncertainties. Consequently, the robust control problem can be defined as a mathematical problem largely depending on the accumulated expertise gained from the measurements, i.e. a knowledge-based control system.

1.2. Modern robust control for T1DM

Although the available T1DM models are all complex nonlinear systems with slowly changing patient parameters over time, the controller has to ensure safety and stability under all circumstances. This means that robustness should be guaranteed. Moreover, there are various constraints and specifications the controller must address complicating the design even further. As the above mentioned control algorithms give individualized solutions leaving robustness a challenge, modern robust control methods seek to provide safety generalized usability with worst case situations handling guarantees. However, increasing robustness will limit tracking properties; hence a robust controller would be inferior to other model-based methods on the nominal model [20].

For this reason, modern robust control, e.g. H_∞ robust controller design can be most effectively used when working with uncertain linear systems [20] with increasing tendency in medical applications as well [21]. In particular, the applicability of this methodology in the T1DM problem has been investigated in [22–24] and the method's advantages have been highlighted in comparison with other control design methods [36–38]. However, a generally applicable method does not exist for nonlinear models, where even proving stability can be a difficult task, and the problem gets more complicated under parameter inaccuracies, uncertainties and unmodeled dynamics.

The *novelty* of the current paper lies on a roadmap of the possibilities and difficulties implementing an H_∞ robust controller for T1DM. For this, one of the reference models of AP researches is used [14], described in Section 2. Section 3 discusses the controller designing aspects. Using the linear parameter varying (LPV) methodology, the nonlinear model is transformed into a linear one without approximation (linearization). Hence, the linear H_∞ control method could be applied on the original nonlinear T1DM model itself. Controllers with different structures and properties are implemented to show robust structure construction particularities, including the selection of weighting functions, robust performance investigation or switching control possibilities, considerations that make the problem a knowledge-based controller design one. The efficiency of the obtained controllers is tested in Section 4 using one of the reference in-silico simulators of the literature, the University of Cambridge SimEdu simulator version 2.2 [25], concluding the results in Section 5.

2. The investigated model

The 11th order model introduced by [10] at Cambridge, UK, represents one of the mostly used T1DM model of the literature for artificial pancreas researches. Later it was updated by [25] leading to University of Cambridge SimEdu simulator used in the current research as well. The model can be described by the following differential equations:

$$\begin{aligned}
\dot{C}(t) &= -k_{a,\mathrm{int}}C(t) + \frac{k_{a,\mathrm{int}}}{V_G}Q_1(t)\\
\dot{Q}_1(t) &= -\left(\frac{F_{01}^s}{Q_1(t)+V_G} + x_1(t)\right)Q_1(t) + k_{12}Q_2(t)\\
&\quad -R_{cl}\max\{0, Q_1(t) - R_{th}V_G\}\\
&\quad +EGP_0\max\{0, 1-x_3(t)\} + U_G(t) - Phy(t)\\
\dot{Q}_2(t) &= x_1(t)Q_1(t) - (k_{12}+x_2(t))Q_2(t)\\
\dot{x}_1(t) &= -k_{b1}x_1(t) + S_{IT}k_{b1}I(t)\\
\dot{x}_2(t) &= -k_{b2}x_2(t) + S_{ID}k_{b2}I(t)\\
\dot{x}_3(t) &= -k_{b3}x_3(t) + S_{IE}k_{b3}I(t)\\
\dot{I}(t) &= \frac{k_a}{V_I}S_2(t) - k_eI(t)\\
\dot{S}_2(t) &= -k_aS_2(t) + k_aS_1(t)\\
\dot{S}_1(t) &= -k_aS_1(t) + u(t)
\end{aligned} \tag{1}$$

where the state variables are:

- $C(t)$ the glucose concentration in the subcutaneous tissue [mmol/L];
- $Q_1(t)$ and $Q_2(t)$ the masses of glucose in accessible and non-accessible compartments [mmol];
- $x_1(t)$, $x_2(t)$ and $x_3(t)$ remote effect of insulin on glucose distribution, disposal and endogenous glucose production respectively [1/min];
- $I(t)$ insulin concentration in plasma [mU/L];
- $S_1(t)$ and $S_2(t)$ insulin masses in the accessible and non-accessible compartments [mU].

The $u(t)$ injected insulin flow of rapid-acting insulin [mU/min] is the input of the system, while the $U_G(t)$ glucose flux from

the gut [mmol/min], and the $Phy(t)$ effect of physical activity [mmol/min] are considered as disturbances.

The parameters of the model are as follows:

- $k_{a,int}$ transfer rate constant between the plasma and the subcutaneous compartment [1/min];
- V_G distribution volume of glucose in the accessible compartment [L];
- F^s_{01} parameter of the total non-insulin dependent glucose flux [mmol/min];
- k_{12} transfer rate constant from the non-accessible to the accessible compartment [1/min];
- R_{cl} renal clearance constant [1/min];
- R_{th} glucose threshold [mmol/L];
- EGP_0 endogenous glucose production extrapolated to the zero insulin concentration [mmol/min];
- k_{b1} and k_{b2} deactivation rate constants [L/(mU · min^2)], k_{b3} deactivation rate constant for the insulin effect on endogenous glucose production [L/(mU · min)];
- S_{IT}, S_{ID} and S_{IE} insulin sensitivities for transport, distribution and endogenous glucose production [L/(mU · min)] and [L/(mU)];
- k_a insulin absorption rate constant [1/min];
- V_I volume of distribution of rapid-acting insulin [L];
- k_e fractional elimination rate from plasma [1/min].

Out of these parameters, the following ones are time-varying: $k_{a,int}$, F^s_{01}, k_{12}, EGP_0, k_{b1}, k_{b2}, k_{b3}, S_{IT}, S_{ID}, S_{IE}, k_a and k_e [14, 25].

The model (1) could be extended with realistic sensor dynamics; however this will not be addressed in this paper for reasons of simplicity. CGM will be modeled with additive white noise. The reason being is that the CGM signal has significant random walk; therefore, an advanced filter or estimator is needed to provide accurate readings to the controller. This is not the scope of this paper, but effective methods can be found in [26, 39].

Six parameter sets representing six different virtual patients were available by the SimEdu in-silico simulator version 2.2, and has been used in the paper for controller design and simulation. SimEdu represents one of the reference in-silico simulators in the artificial pancreas (AP) researches developed in accordance with FDA regulations [25].

3. Controller design

The H_∞ control methodology has been established for linear systems [20]. As T1DM models are nonlinear, an important issue is the direct non-linearized applicability in the control scheme taking the parameter inaccuracies into consideration as well.

3.1. LPV modeling

There are several ways to handle the nonlinearity of the model. The classical nonlinear methodology focuses on a differential geometric approach [27], while a more recent methodology is represented by linear parameter varying (LPV) systems [28–29].

LPV is an acceptable compromise between the model's complexity and the developed control algorithm, as LPV systems can be seen as an extension of linear time invariant (LTI) systems, where the relations are considered to be linear, but model parameters are assumed to be functions of a time-varying signal [29]:

$$\begin{aligned}\dot{x}(t) &= A(\rho(t))x(t) + B(\rho(t))u(t)\\ y(t) &= C(\rho(t))x(t) + D(\rho(t))u(t)\end{aligned} \tag{2}$$

where:

$$A(\rho(t)) = \prod_{i=1}^{m} \rho_i(t)A_i \qquad B(\rho(t)) = \prod_{i=1}^{m} \rho_i(t)B_i$$

$$C(\rho(t)) = \prod_{i=1}^{m} \rho_i(t)C_i \qquad D(\rho(t)) = \prod_{i=1}^{m} \rho_i(t)D_i \tag{3}$$

It can be observed that (2) is an LTI system in the $\rho(t)$ scheduling parameters; hence nonlinearity can be hidden and the A, B, C, D matrices in (3) should be treated correspondingly during control design [29].

One approach could be the linearization around stable working points in the state-space, then creating a polytopic region of possible linear models, and using this information to determine the nominal model and uncertainty weighting functions [23]. The current paper can be considered as a continuation of the article presented in [23], in a more rigorous and complex manner. As in [23] only a given scenario was analyzed to present the capability of LPV-modeling for T1DM control (i.e. for a given parameter set a robust controller has been designed), here we give a complex roadmap of the nonlinear robust control design for T1DM, analyzing different parameter possibilities and highlighting the sensitivity of uncertainty weighting function selection. Based on the gained knowledge from real patient data collected from insulin pump centers (clinics and hospitals affiliated to the Hungarian Diabetes Association and considered the only legal entities in Hungary to work with CGMS and insulin pumps) we could formulate the weighting functions of the neglected uncertainties of the model.

Beyond the polytopic representation, the other most widely used LPV-modeling approach exploits the affine representation (similar to quasi-Affine LPV) of the nonlinear model [30]. Given a bounded vector $\rho(t)$ with bounded time-derivatives, the model can be treated as a linear model with parameter inaccuracies. For the model (1) all candidates $\rho(t)$ (named as scheduling parameters) are given in (4), being bounded (5-6) with their time-derivatives as well [37]. Numerical values were determined analytically and validated with Monte-Carlo simulations [37].

$$\rho(t) = \begin{pmatrix} Q_1(t) & \frac{F^s_{01}}{Q_1(t)+V_G} & Q_2(t) & x_1(t) & x_2(t)\end{pmatrix}^T \tag{4}$$

where:

$$\rho_{\min} = \begin{pmatrix} Q_{1,\min} & \frac{F^s_{01}-\Delta F^s_{01}}{Q_{1,\max}+V_G} & Q_{2,\min} & x_{1,\min} & x_{2,\min}\end{pmatrix}^T \tag{5}$$

$$\rho_{\max} = \begin{pmatrix} Q_{1,\max} & \frac{F^s_{01}+\Delta F^s_{01}}{Q_{1,\min}+V_G} & Q_{2,\max} & x_{1,\max} & x_{2,\max}\end{pmatrix}^T \tag{6}$$

The existence of a qALPV model would make LPV-based control possible. From the proposed members of $\rho(t)$ parameters however none can be measured; therefore, an LPV-based controller cannot be implemented directly. Instead, the bounds should be used as parameter inaccuracies of a linear model leading to two possible approaches:

- Define an uncertain model directly;
- Create input and output multiplicative uncertainties.

For the current T1DM model the latter option was chosen easing the extension of unstructured uncertainties. Furthermore, the decision was influenced by the twelve time varying parameters of the model ($k_{a,int}$, F^s_{01}, k_{12}, EGP_0, k_{b1}, k_{b2}, k_{b3}, S_{IT}, S_{ID}, S_{IE}, k_a and k_e – see *Section 2*).

However, the choice of parameters for the qALPV-like description is not a trivial task. Finding the correct model can greatly reduce the burden on the controller, while choosing a wrong configuration could lead us to an overly complicated problem, where the performance of the controller could be similar to the performance of a classical control strategy.

Introducing $\mu_i \in [0, 1]$ $(i = 1, \ldots, 4)$ parameters to investigate different configurations, while $\delta_i \in [0, 1]$ represent parameter inaccuracies, including the changing of scheduling parameter

candidates, the state-space model of the system is described in Appendix A in which Δ reflects the variation of the parameter uncertainties (a variation of 5% was considered in each case as suggested in [25]).

After evaluating all possible scenarios the configuration (μ_1, μ_2, μ_3, μ_4)=(0, 0, 0, 0) was chosen. This means that state variables $x_1(t)$ and $x_2(t)$, the remote effect of insulin on glucose distribution and disposal, are not considered part of $\rho(t)$, while the switching effect of the endogenous glucose production ($x_3(t)$) is considered as disturbance only. The reasons behind this choice are as follows:

- Although all of $Q_1(t)$, $Q_2(t)$, $x_1(t)$ and $x_2(t)$ states of the model (1) are bounded, the bounds of $Q_1(t)$ and $Q_2(t)$ only depend on the performance of the controller. Smaller the glucose level region the controller can keep, the smaller the parameter inaccuracy of the model. On the other hand $x_1(t)$ and $x_2(t)$ are bounded by the amount of injected insulin flow. Higher the maximal value of the possibly administered insulin, the faster the controller disturbance compensation. Moreover, to avoid hypoglycemia, zero insulin flow is a possible scenario as well. For better control properties, wider limits for the input are needed, but at the same time the effect of parameter inaccuracies will also grow;
- It can be easily demonstrated that $\mu_1 = 0$ will slow the dynamics of $Q_1(t)$ in the nominal model, but at the same time the effect of the input will be the largest. On the other hand, $\mu_1 = 1$ would mean that the insulin concentration has no direct effect on the plasma glucose levels;
- The reason behind choosing $\mu_3 = 0$ and the effects of insulin on $Q_2(t)$ is the same with μ_1 and $Q_1(t)$ discussed previously;
- In case of μ_2, choosing $Q_1(t)$ as parameter over $x_1(t)$ will leave the insulin dynamics having an opposite effect on $Q_2(t)$ (the rise in $I(t)$ would increase the value of Q_2(t)). Choosing a non-zero value for μ_2 however will lead to complex conjugate pole pairs in the nominal model, with possibly instable dynamics depending on the actual value of the $\rho(t)$ vector;
- Choosing $\mu_4 = 1$ would definitely raise the effect of the injected insulin on the controller, but the inaccuracy of the model would also increase. Moreover, the controller has no information on the fact that the state variable $x_3(t)$ and the endogenous glucose production is connected.

3.2. Weighting functions

Weighting functions and unstructured uncertainty blocks represent effective tools to incorporate our a priori knowledge of the controlled process into the model that is used for controller design. Unstructured uncertainty blocks represent linear systems with bounded norm (H_∞ norm ≤ 1 in this particular case) and unknown but stable and minimal phase dynamics [20]. Furthermore, various constraints can be represented with weighting functions, such as control signal limitations, tracking performance and disturbance rejection. Once a model has been constructed in such manner, computing the parameters of the corresponding controller becomes a convex optimization problem. This is definitely one of the greatest advantages of modern robust controllers and it requires a deep understanding of the process dynamics (in our case the T1DM) obtained mostly from measurements. In our case, the gained knowledge and hence, the understanding of the diabetic patient behavior came from 83 patients' more than 200 week continuous glucose datasets analyzed throughout the years and collected from the insulin pump centers of the Hungarian Artificial Pancreas Working Group created in collaboration with the Hungarian Diabetes Association [40–41].

For classical control methods (e.g. PID) and nowadays frequently used modern MPC method, synthesis is relatively easy for the nominal model. However, when the above mentioned constrains, uncertainties and disturbances are present satisfying all of them is impossible (e.g. PID controller) or requires solving nonlinear optimization tasks with demanding numerical methods (e.g. MPC). A working controller can be implemented nevertheless, but safety cannot be guaranteed.

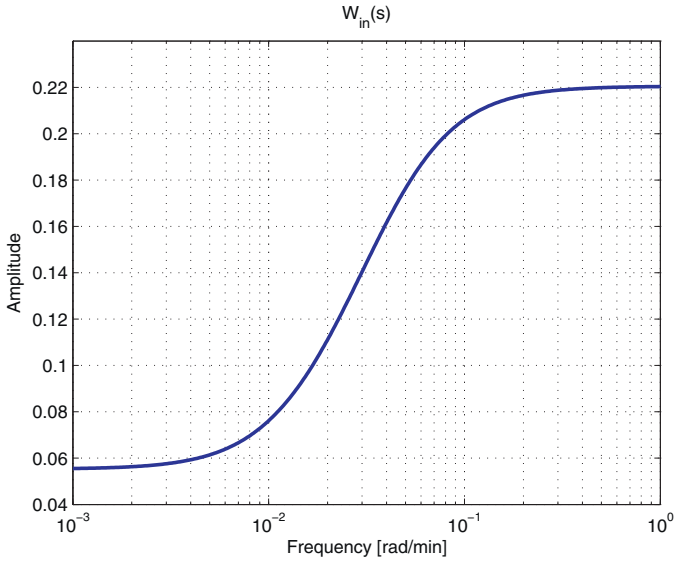

Fig. 1. Frequency characteristic of the weighting function $W_{in}(s)$.

Using the parameter inaccuracy information and the LPV-model constructed above, uncertainty weighting functions can be determined. There are altogether four of these functions: $W_{in}(s)$, $W_1(2)$, $W_2(s)$ and $W_{out}(s)$. The transfer functions were determined based on gridding technique and upper approximation of the frequency responses obtained, similar to [31]. The results are based on the six patients' simulations of SimEdu in-silico simulator [25].

$W_{in}(s)$ represents the uncertainty of the dynamics of the subsystem (denoted as $G_1(s)$ later) of (1) consisting of the state variables $S_1(t)$, $S_2(t)$ and $I(t)$. Its transfer function is presented in (7), while the amplitude spectrum is displayed in Fig. 1. At smaller frequencies, the uncertainty remains 5.5%, while it rises up to 22% for frequencies larger than 0.1 rad/min [31].

$$W_{in}(s) = 0.055\frac{101.01s+1}{25.31s+1} \tag{7}$$

$W_1(s)$, $W_2(s)$ represent the uncertainty of $x_1(t)Q_1(t)$ and $x_2(t)Q_2(t)$ output of the subsystem containing state variables $x_1(t)$, $x_2(t)$ and $x_3(t)$ (referred to as $G_2(s)$). This includes the effect of the changing parameters and the change of the selected scheduling parameters. The chosen transfer functions of these weights are presented in (8), while their amplitude spectrum is displayed in Fig. 2 and Fig. 3. All values were determined by the same gridding technique [31], except that here both model parameter and scheduling parameter changes were considered. $W_2(s)$ is significantly larger than $W_1(s)$ since $x_2(t)$ varies in wider range. Furthermore, the parameters of $W_2(s)$ are different for each of the six patient of SimEdu [25], while one common $W_1(s)$ is used. K, T and τ are parameters.

$$W_1(s) = 0.536\frac{714s+1}{624s+1}$$
$$W_2(s) = K\frac{\tau s+1}{Ts+1} \tag{8}$$

Finally $W_{out}(s)$ was chosen as presented in (9) and Fig. 4. In the subsystem ($G_1(s)$) consisting of state variables $C(t)$, $Q_1(t)$ and $Q_2(t)$ there are various uncertain parameters, a scheduling variable,

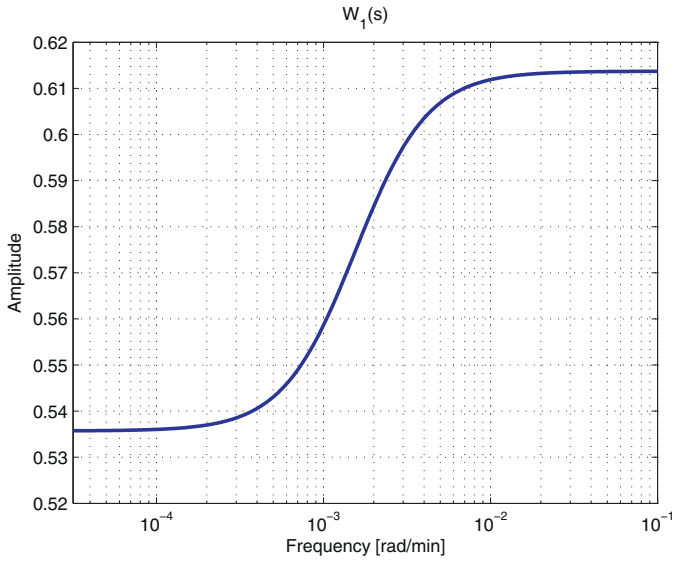

Fig. 2. Frequency characteristic of the weighting function $W_1(s)$.

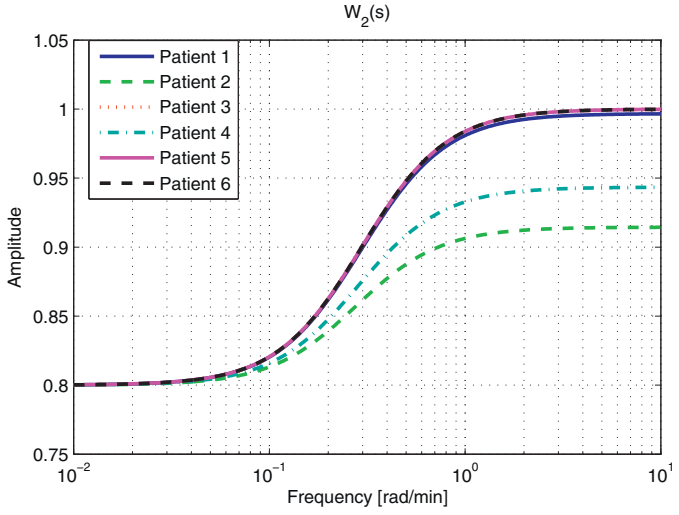

Fig. 3. Frequency characteristic of the weighting functions of $W_2(s)$.

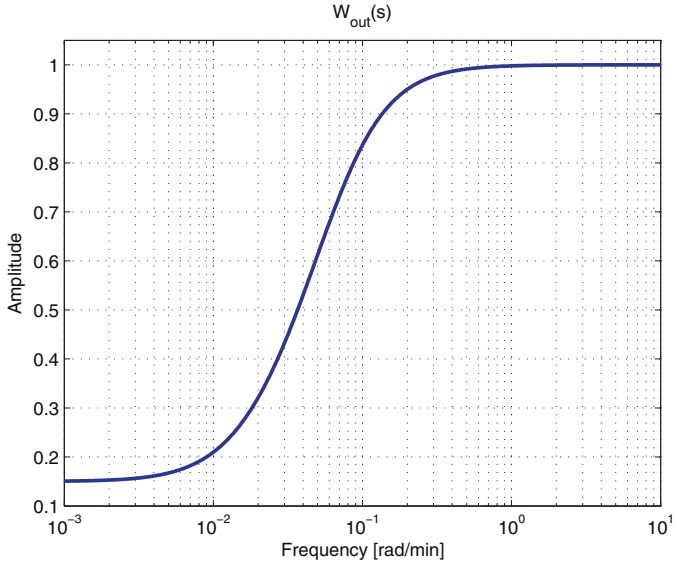

Fig. 4. Frequency characteristic of the weighting function $W_{out}(s)$.

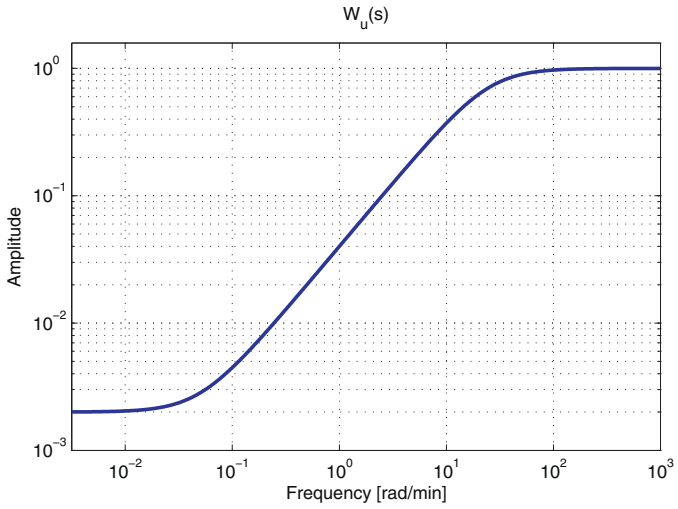

Fig. 5. Frequency characteristic of the weighting function $W_u(s)$.

as well as a kind of switching effect because of renal clearance: $R_{cl}\max\{0, Q_1(t) - R_{thr}V_G\}$. The other switching component representing endogenous glucose production ($EGP_0\max\{0, 1 - x_3(t)\}$) is treated as noise in accordance with what was presented earlier as gained knowledge about the nominal model. On higher frequencies the amplitude goes up to one, which represents 100% uncertainty. This represents the assumption that we have no reliable information on the behavior of the system on frequencies close to the sampling frequency; furthermore there might be neglected dynamics.

$$W_{out}(s) = 0.15\frac{100s+1}{15s+1} \tag{9}$$

The disturbances also require weighting functions. $W_m(s)$ for the glucose flux from the gut is created using the meal absorption model presented in [25]. Although it is nonlinear in the original model, a worst case representation is possible with a second order linear system:

$$W_m(s) = \frac{U_{G,ceil}}{(t_{\max}s+1)^2} \tag{10}$$

where $U_{G,ceil}$ is the maximum glucose flux from the gut [mmol/kg/min], while t_{max} is the time-to-maximum appearance rate of glucose in the accessible compartment [min].

The effect of physical activity does not need an additional component aside from a corresponding input. The measurement noise has a constant weighting function: $W_n = 0.5$ representing 0.5 mmol/L standard deviation of the measurement noise [37].

The constraints on the control signal can also be captured with a weight. It can be either constant with value $W_u = u_{\max}^{-1}$, or we can also restrict fast changes with a transfer function presented in Fig. 5. Limiting the control signal on higher frequencies can prevent rapid oscillations.

Finally, we have to define the desired tracking performance with a weighting function denoted as $W_p(s)$. Using our gained knowledge in the field [37, 42], our choice in this particular case is presented by a first order system given in (11). The numerical values are different for every controller, but the structure remains the same in a sense that the requirements are different for lower and higher frequencies. The former drives the glucose concentration towards the normoglycemic range, while the latter gives more relaxed bounds on rapid changes. This is in accordance with the uncertainty of the model in high-frequency regions. Furthermore, oscillations and hypoglycemic episodes can be reduced at the cost

Table 1
Parameters of performance weighting functions.

Controller	T	τ	K
Regular (low γ)	300	9.6774	0.031
Regular (high γ)	350	7.7778	0.045
Integral (low γ)	400	40	0.01
Integral	300	30	0.05
2DoF (low γ)	400	16	0.025
2DoF (high γ)	300	30	0.05
Integral 2DoF (low γ)	400	40	0.01
Integral 2DoF (high γ)	300	30	0.05

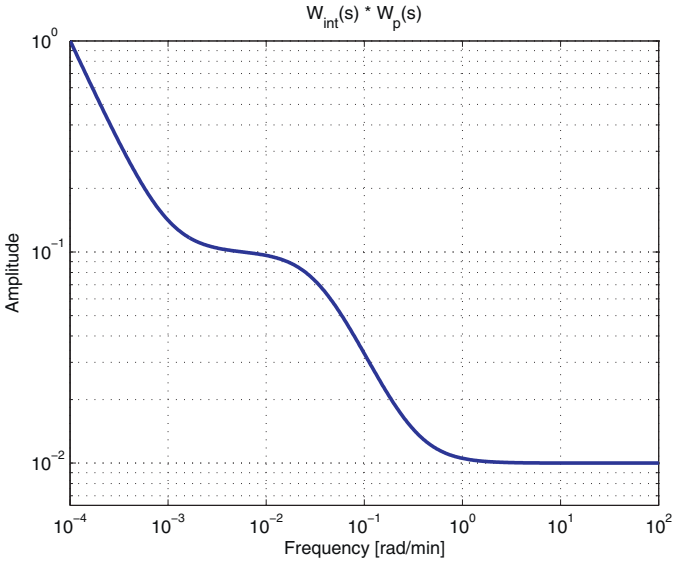

Fig. 6. Example for complete weighting functions of $W_{int}(s)$ and $W_p(s)$.

of longer hyperglycemic events.

$$W_p(s) = K\frac{\tau s + 1}{Ts + 1} \tag{11}$$

The numerical values for each controller are summarized in Table 1. Note that there are two versions for each controller. The reasons will be explained later in *Section 3.3*.

As an example, choosing 0.5 for low frequencies means that the residual tracking error should be lower than 2 mmol/L even in the most extreme case.

In classical control theory PID control or controllers containing an integrator can effectively eliminate residual error, which is a useful property when dealing with uncertain systems. However, in H_∞, control performance weighting functions cannot contain integrator, for it has infinitely large H_∞ norm, but we can make it part of the model in a different manner (as shown later in Fig. 10 and Fig. 12). In this case, the additional $W_{int}(s)$ component could be defined with a transfer function given in (12), determined on the responses of the SimEdu virtual simulator [25]. The output of $W_{int}(s)$ must be made available for measurement. The series of this element with the performance weight function $W_p(s)$ can result in an amplitude spectrum similar to the illustration presented in Fig. 6.

$$W_{\text{int}}(s) = \frac{1000s + 1}{1000s} \tag{12}$$

Furthermore, a two degree of freedom (2DoF) control structure is also possible. In order to achieve this, we require a reference system $W_{track}(s)$. Instead of following a reference signal directly, the aim was to match the behavior of the controlled system to the reference system. In case of a classical 2DoF control the controller consists of a feed-forward and feedback component, where

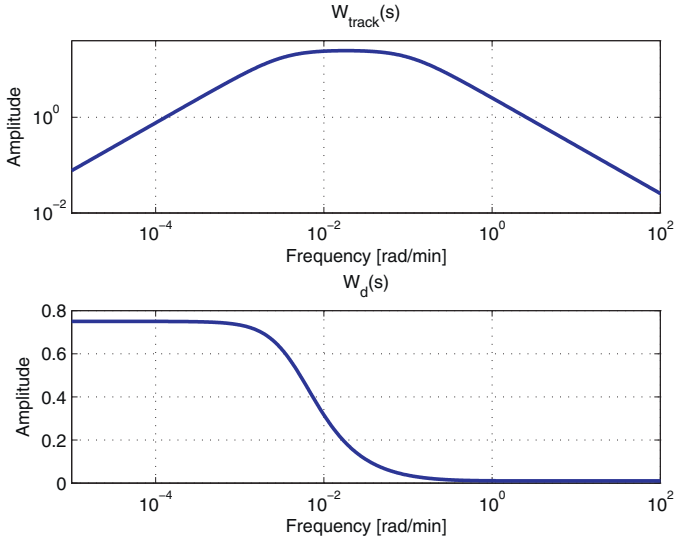

Fig. 7. Frequency characteristic of the weighting functions of $W_{track}(s)$ and $W_d(s)$.

the former acts as a filter of the reference signal. Since the reference signal in this case is constant, the feed-forward component is not needed.

However, we do require an adequate estimation of the disturbances affecting the model, for which the reference model responds with desired behavior. Hence, the controller in the 2DoF model will provide an estimation of the output of $W_m(s)$ with estimation error constrained by weighting function $W_d(s)$. Only the meal disturbance was considered, since this has the most significant impact on the blood glucose levels among the processes that always elevate the glucose concentration. Endogenous glucose production is assumed to change rapidly because of the switching effect; hence, it is difficult to observe in these settings. The transfer functions of $W_{track}(s)$ and $W_d(s)$ are presented in (13) and displayed on Fig. 7 and determined on simulations of SimEdu's responses (based on all the responses an upperbound function was determined empirically). Note that the output of $W_m(s)$ is divided by U_G before entering $W_d(s)$.

$$W_{track}(s) = \frac{76500s}{3000s^2 + 310s + 1}$$
$$W_d(s) = 0.75\frac{2.86s + 1}{215s + 1} \tag{13}$$

3.3. Controller structure

The controller structures for regular controller, integral control, 2DoF control and 2DoF with integrator are presented on Fig. 8 including all the uncertainty weighting functions determined above. The components with solid line are common for all types and the weighting functions described above. In case of 2DoF control, the elements drawn with dashed line should be also taking into account, including the tracking performance weighting function $W_p(s)$, the $W_d(s)$ for output estimation of $W_m(s)$ and the reference system $W_{track}(s)$. Dotted line marks the parts that belong to integral control ($W_{int}(s)$ and a separate tracking performance function $W_p(s)$), as opposed to the semi-dotted elements that are present only in the absence of the integrator.

The components $W_{in}(s)$, $W_1(s)$, $W_2(s)$, $W_{out}(s)$, $W_m(s)$, $W_n(s)$, $W_u(s)$, $W_p(s)$, $W_{int}(s)$, $W_d(s)$ and $W_{track}(s)$ were introduced previously. $G_1(s)$, $G_2(s)$ and $G_3(s)$ stand for the subsystems described when the uncertainty weighting functions were presented. The controller provides the injected insulin control signal $u(t)$ and estimated disturbance $\hat{d}(t)$ in the 2DoF case. The disturbances are

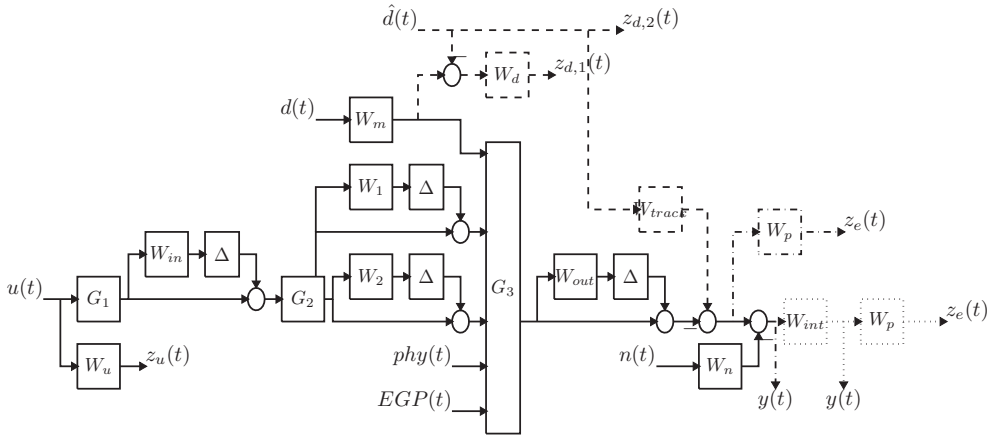

Fig. 8. Considered structures of the H_∞ controllers.

the ingested meal *d(t)*, effect of physical activity *phy*(t), sensor noise *n(t)*, and the disturbance resulting from endogenous glucose production *EGP(t)*. $z_e(t)$ and $z_u(t)$ are outputs of the performance weighting functions, while $z_{d1}(t)$ and $z_{d2}(t)$ keep the disturbance estimation in check. $y(t)$ is the measured output of the system.

Note that the reference signal cannot be found in Fig. 8. The reason is that the reference signal is constant, and no constant input of the model has significance when designing a linear dynamic system. The offset caused by the reference signal, or other elements of the model is compensated by the integrator if present, otherwise an additional constant input is needed.

An additional safety feature has been included in all controllers. Whenever the measured blood glucose concentration reaches a certain lower limit (4.5 mmol/L), the control signal will be set as zero. This is a frequently used method in recent insulin pumps avoiding or reducing certain hypoglycemic episodes. The controller could be tuned to avoid these episodes without using this feature, if the uncertainty of the model would not be this high. However, the reason of high uncertainty used in this paper was to iterate on the possibilities in modern robust controller design, giving a roadmap of it.

The controllers were implemented using Robust Control Toolbox of MATLAB 2009b.

The current case study highlights the difficulties in order to assure robust performance (RP), i.e. an H_∞ norm smaller than one for the transfer matrix of the closed loop system. This can only be satisfied by defining weak tracking performance, inadequate to keep the plasma glucose concentration of the patient in the normoglycemic range.

Therefore, two different versions were considered for each controller: one where RP is met and one where only robust stability (RS) is assured. The latter has stricter performance specifications, which are not met, but closed loop stability is still ensured. (Needless to say, a true solution would reduce the uncertainties of the system, but this cannot be done with a linear controller.)

One very important feature of this control strategy is that no information regarding the occurrence and size of meals is provided,

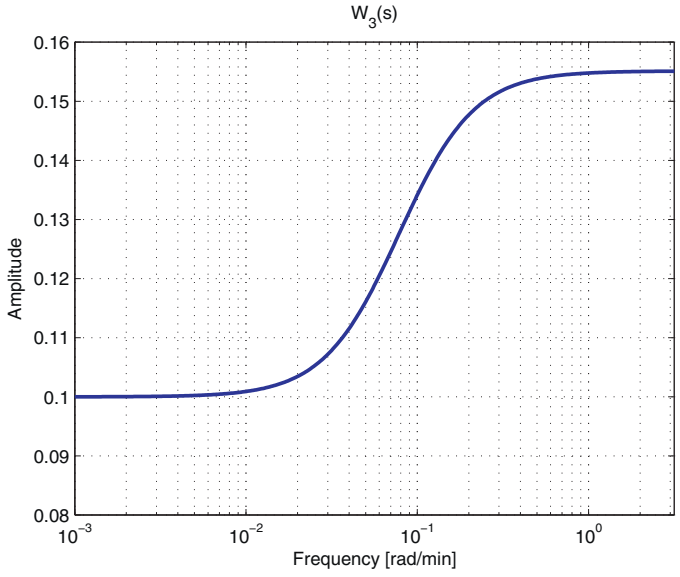

Fig. 9. Frequency characteristic of the weighting function $W_3(s)$.

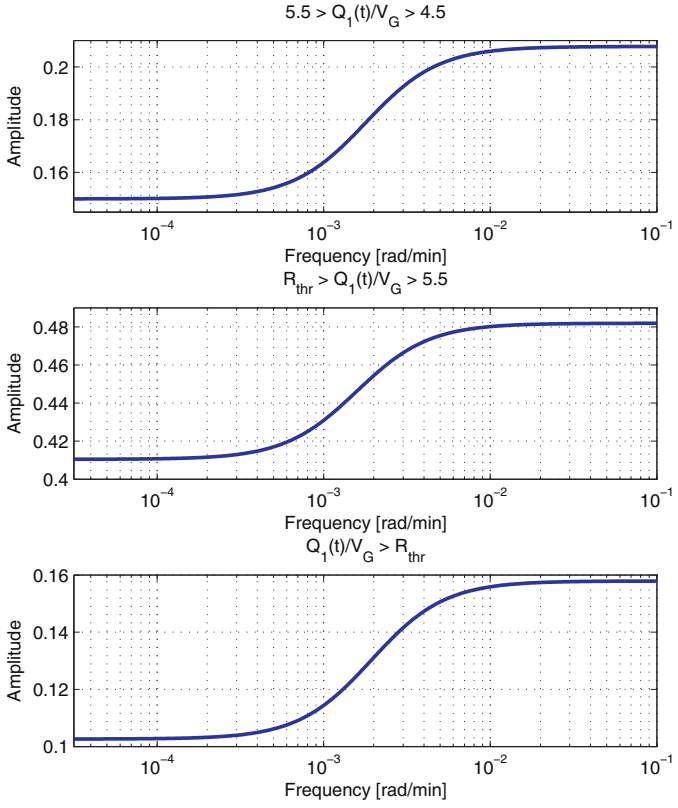

Fig. 10. Weighting functions of $W_1(s)$ in switching controller.

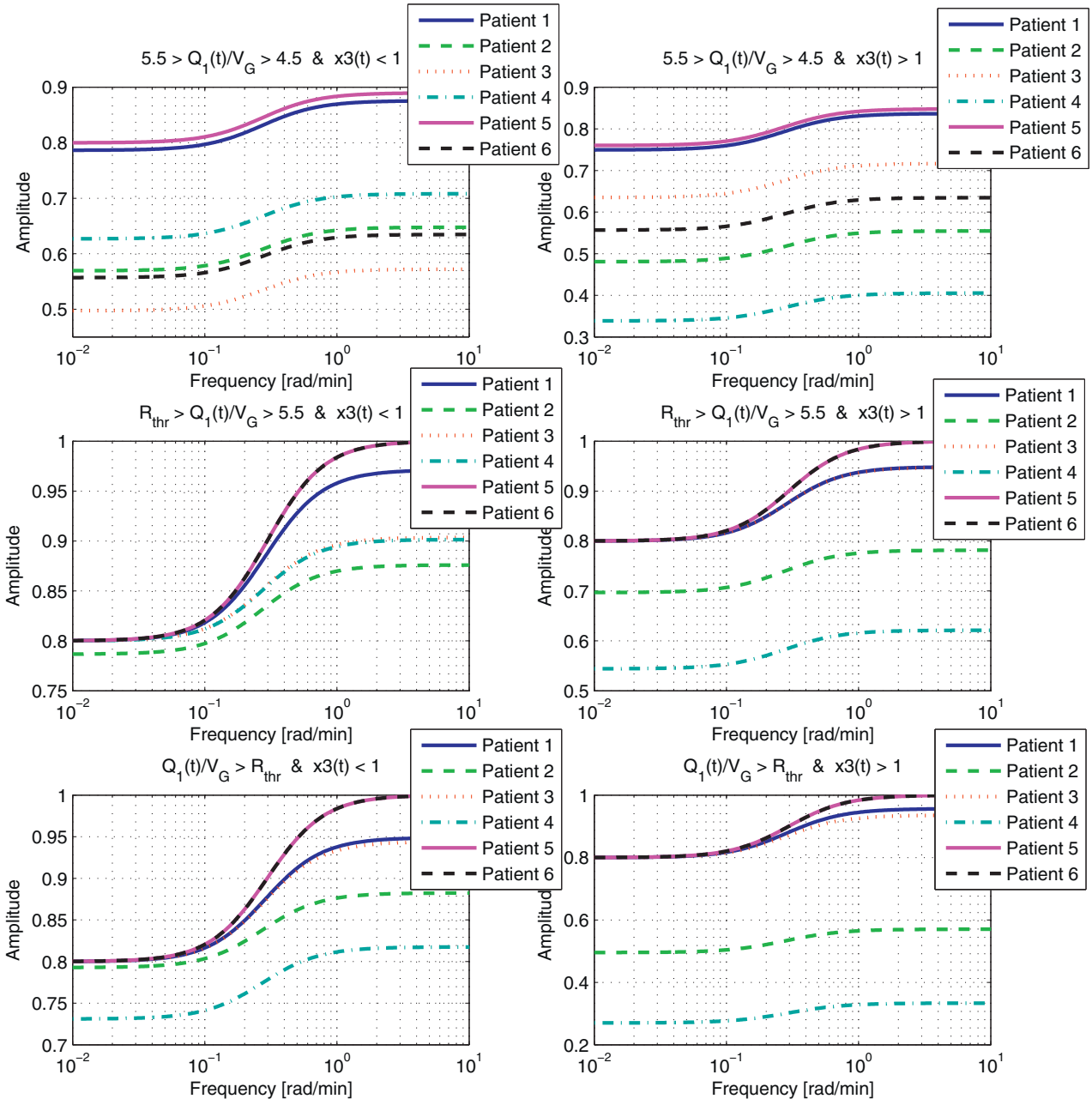

Fig. 11. Weighting functions of $W_2(s)$ in switching controller.

unlike many other methods found in the literature. This certainly leaves a great burden on the controller, but makes it significantly less dependent from the compliance of the patient and approaches better the real life situation of a diabetic patient.

3.4. Switching control

A more effective approach can take into consideration the "switching" nature of the model. Endogenous glucose production (*EGP*) and renal clearance (R_{cl}) represent linear dependencies in certain working points, and non-existent in others. Treating each case separately four different models can be defined requiring four different controllers. Each model has slightly different dynamics, but individually they impose less burden on the respective controllers. Furthermore, based on the blood glucose levels more models can be defined, similar to [32]. The six considered models are:

- No *EGP(t)* and $Q_1(t) \in [4.5 \cdot V_G, 5.5 \cdot V_G]$ (no renal clearance);
- *EGP(t)* is active, $Q_1(t) \in [4.5 \cdot V_G, 5.5 \cdot V_G]$ (no renal clearance);
- No *EGP(t)* and $Q_1(t) \in (5.5 \cdot V_G, R_{th}V_G]$ (no renal clearance);
- *EGP(t)* is active, $Q_1(t) \in (5.5 \cdot V_G, R_{th}V_G]$ (no renal clearance);
- No *EGP(t)* and $Q_1(t) > R_{th}V_G$ (renal clearance active);
- *EGP(t)* is active, $Q_1(t) > R_{th}V_G$ (renal clearance active).

Unfortunately the state variables that could be used to perform the switching cannot be measured, only estimated. The structure of the nominal model and the controllers are the same as previously, except that *EGP(t)* is not a disturbance anymore, but part of the system. This calls for an additional uncertainty weighting function $W_3(s)$ given in (14), which incorporates the parameter changes of k_{b3} and S_{IE} (Fig. 9). Similarly to $W_1(s)$ and $W_2(s)$ the parameters of $W_3(s)$ were determined by gridding technique [31].

$$W_3(s) = 0.0627\frac{17.7904s + 1}{11.468s + 1} \tag{14}$$

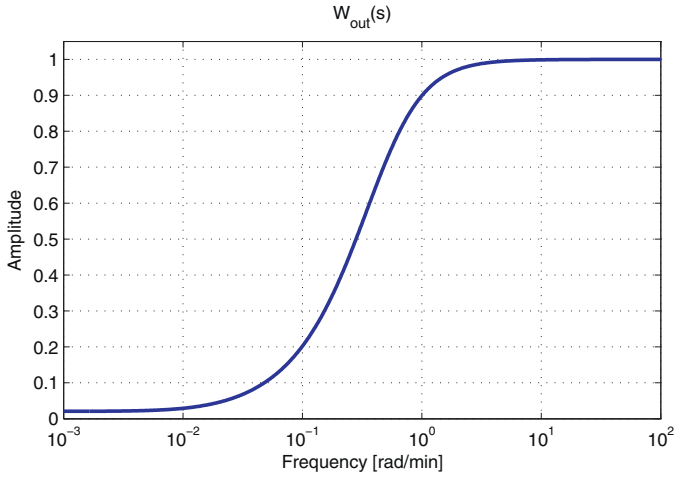

Fig. 12. Weighting function $W_{out}(s)$ in switching controller.

Table 2
Parameters of performance weighting functions for switching controllers.

Controller	T	τ	K
Regular ($4.5 < Q1(t)/V_G \leq 5.5$) (low γ)	300	37.5	0.04
Regular ($5.5 < Q1(t)/V_G \leq R_{th}$) (low γ)	300	50	0.03
Regular ($R_{th} < Q1(t)/V_G$) (low γ)	300	33.33	0.045
Regular ($4.5 < Q1(t)/V_G \leq 5.5$) (high γ)	300	6	0.05
Regular ($5.5 < Q1(t)/V_G$) (high γ)	300	5	0.06
Integral (low γ)	400	40	0.01
Integral ($4.5 < Q1(t)/V_G \leq 5.5$) (high γ)	300	30	0.05
Integral ($5.5 < Q1(t)/V_G \leq R_{th}$) (high γ)	300	25	0.06
Integral ($R_{th} < Q1(t)/V_G$) (high γ)	300	21.43	0.07
2DoF ($4.5 < Q1(t)/V_G \leq 5.5$) (low γ)	300	9.375	0.032
2DoF ($5.5 < Q1(t)/V_G \leq R_{th}$) (low γ)	300	10	0.03
2DoF ($R_{th} < Q1(t)/V_G$) (low γ)	300	8.57	0.035
2DoF (high γ)	300	12	0.05
Integral 2DoF ($4.5 < Q1(t)/V_G \leq 5.5$) (low γ)	300	30	0.01
Integral 2DoF ($5.5 < Q1(t)/V_G \leq R_{th}$) (low γ)	400	40	0.01
Integral ($R_{th} < Q1(t)/V_G$) 2DoF (low γ)	300	12	0.025
Integral 2DoF ($4.5 < Q1(t)/V_G \leq 5.5$) (high γ)	300	30	0.05
Integral 2DoF ($5.5 < Q1(t)/V_G \leq R_{th}$) (high γ)	300	7.5	0.04
Integral 2DoF ($R_{th} < Q1(t)/V_G$) (high γ)	300	23.077	0.065

By the mentioned considerations on switching, the uncertainty will be reduced for certain components of the model. Furthermore different weighting functions can be defined for different working points and also for different patients. $W_1(s)$ differs depending on the value of $Q_1(t)$ resulting in three different weights given as follows (Fig. 10).

$$W_1(s|4.5 < Q_1(t)V_G \leq 5.5) = 0.15\frac{714.286s+1}{515.724s+1} \tag{15}$$

$$W_1(s|5.5 < Q_1(t)V_G \leq R_{th}) = 0.41\frac{714.286s+1}{608.415s+1} \tag{16}$$

$$W_1(s|R_{th} < Q_1(t)V_G) = 0.103\frac{714.286s+1}{464.28s+1} \tag{17}$$

Based on the remarks given at $W_2(t)$ selection, i.e. the parameters of $W_2(s)$ are different for each of the six patient of SimEdu (see Eq. (8) and Fig. 3), for every switching case a corresponding frequency evaluation of $W_2(t)$ is required (Fig. 11).

On the other hand, based on (9), the $W_{out}(s)$ weighting function represents smaller uncertainty on lower frequencies (Fig. 12).

$$W_{out}(s) = 0.02\frac{2.05s+1}{100s+1} \tag{18}$$

Three mostly different performance weighting function were determined for every controller depending on the value of $Q_1(t)$. The controllers could further be tuned by defining different W_p for every working point. The parameters are summarized in Table 2. The time constant (T) is selected on the model property (only in case of integral control is used a higher time due to meal absorption), K and τ are results of the weighting functions selected.

Similarly to the non-switching case, two different versions have been implemented for each type of controllers: one where RP is satisfied and one where only RS is true. The structures of all four switching controllers are presented in Fig. 13 (similar to Fig. 8, just that here the uncertainty weighting function $W_3(s)$ is included in addition for the endogenous glucose production part), where the line-style of the different elements is the same as in the non-switching case. The components with solid line are common for all types. In case of 2DoF control, the elements drawn with dashed line should be also taken into account. Dotted line marks the parts that belong to integral control, as opposed to the semi-dotted elements that are present only in the absence of the integrator.

All six controllers were implemented and ran in parallel. The control signal will be the weighted sum of all controller outputs. The weights are determined using sigmoid functions to avoid rapid changes in the signal during switching. For a controller that is valid when $Q_1(t) \in [\underline{Q}_{1,i}, \overline{Q}_{1,i}]$ and $x_3(t) \in [\underline{x}_{3,i}, \overline{x}_{3,i}]$ the weight $\tilde{w}_i$ will be determined as follows:

$$w_i = \frac{1}{1+\exp\left(M\left(\underline{Q}_{1,i} - Q_1(t)\right)\right)}\frac{1}{1+\exp\left(M\left(Q_1(t) - \overline{Q}_{1,i}\right)\right)}$$

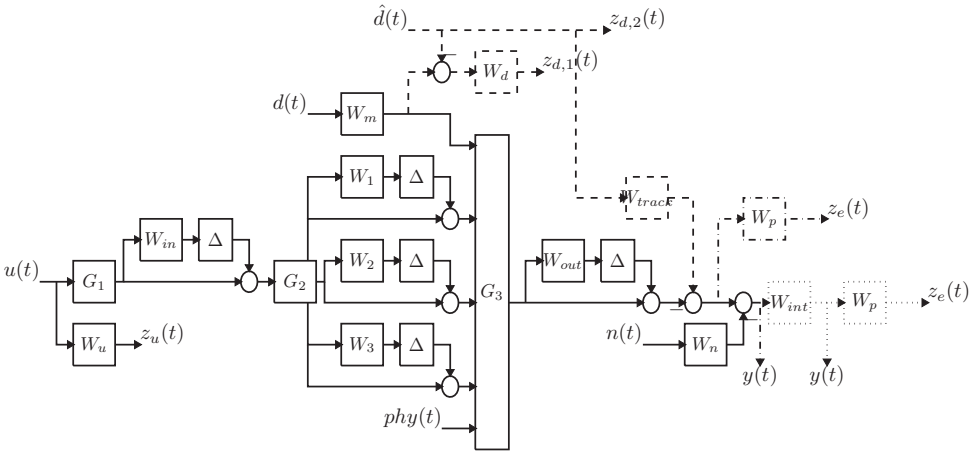

Fig. 13. Considered structures of the switching H_∞ controllers.

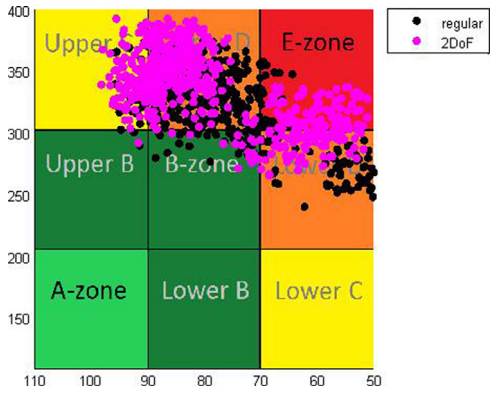

Fig. 14. Control variability grid analysis for controllers without switching (low γ).

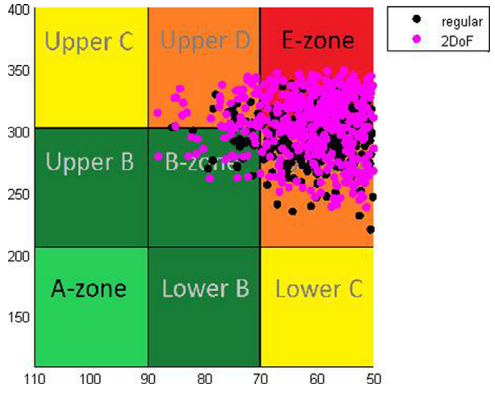

Fig. 15. Control variability grid analysis for controllers without switching (high γ).

$$\times \frac{1}{1+\exp\left(M\left(\underline{x}_{3,i}-x_3(t)\right)\right)}\frac{1}{1+\exp\left(M\left(\overline{x}_{3,i}-x_3(t)\right)\right)} \tag{19}$$

$$\tilde{w}_i = \frac{w_i}{\sum_{j=1}^{6} w_j} \tag{20}$$

The control signal is considered zero when the lower threshold of the measured glucose concentration (4.5 mmol/L) is reached.

Compared to the non-switching case, smaller γ values could be achieved for the same performance functions. On the other hand, the synthesis could become numerically badly conditioned when faster tracking properties have been enforced. Furthermore, the poles of the controller could grow too high, resulting in slow simulations. Consequently, balanced model reduction was necessary [20].

4. Simulation results

Altogether eight different controllers were implemented and tested using the University of Cambridge Simulator educational version 2.2 (SimEdu) [25].

In case of integral control RP was not possible to be achieved with merely reducing the weighting of the tracking performance, and not even RS could be ensured in certain cases. Results include massive hypoglycemic episodes during simulation, which suggests that unless the uncertainty is reduced, or additional information is made available regarding the disturbances (e.g. meal intake), integral control is not favorable for H_∞ control of this model. However, for H_2 or L_1 control the idea might be more effective [20]. PID control is extensively researched for the AP problem [8, 13], therefore

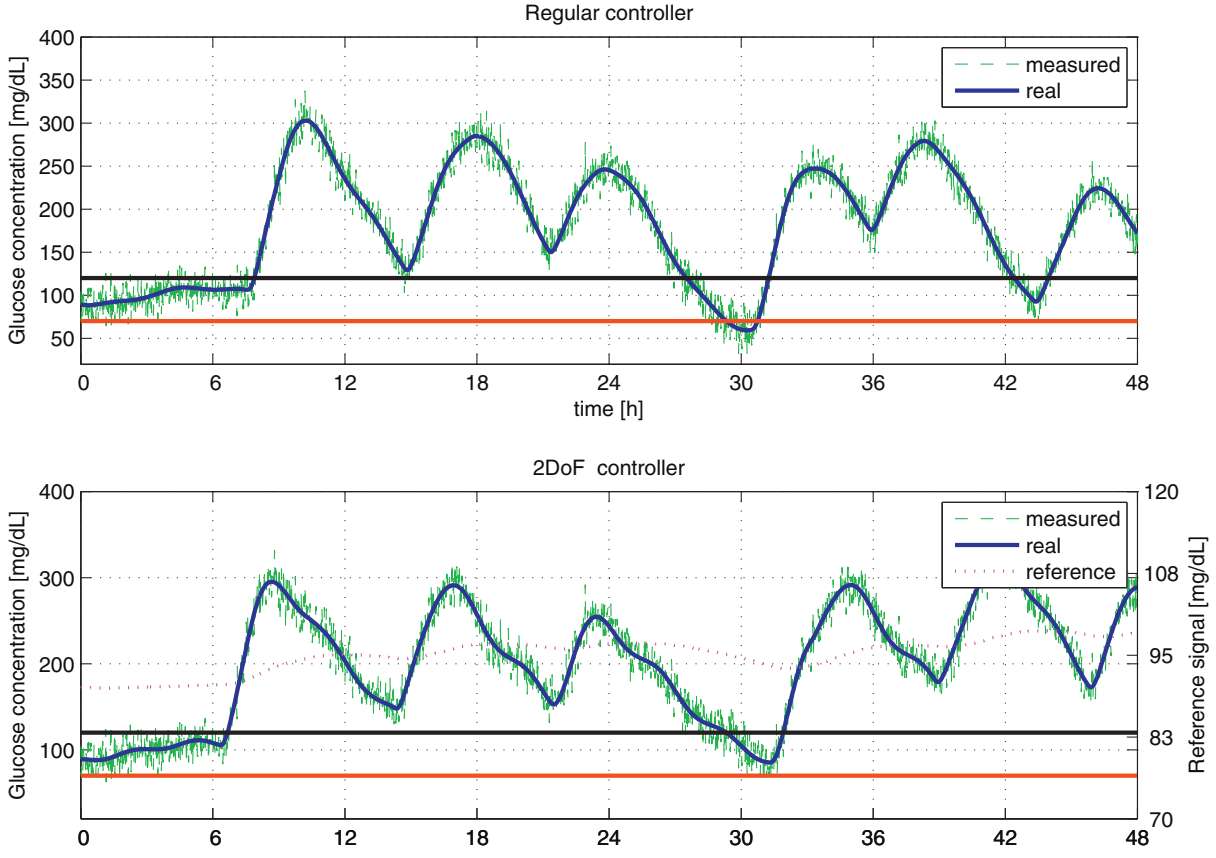

Fig. 16. Simulation over time for non-switching H_∞ controller (low γ). "Measured" represents the signal measured by the CGM sensor, "real" stands for the output of the system, while "reference" is for the output of the reference system W_{track}.

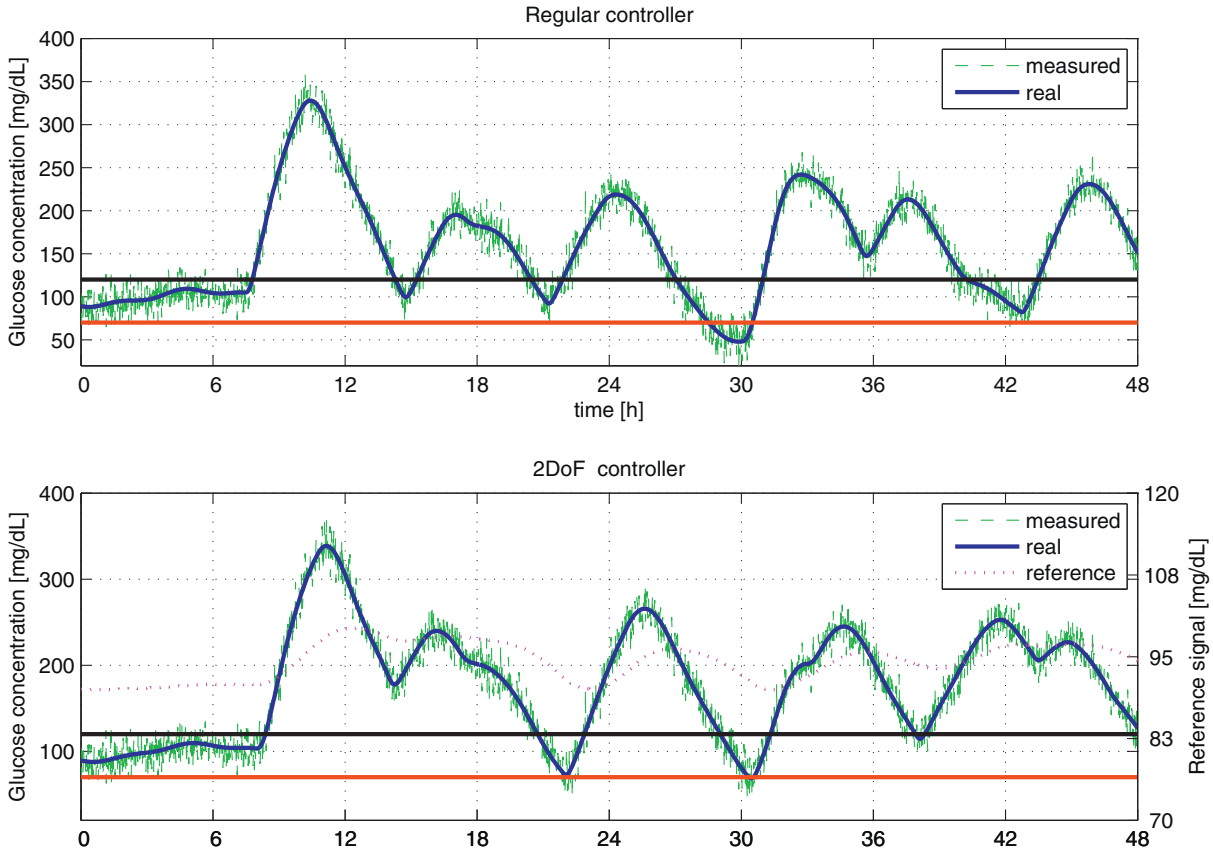

Fig. 17. Simulation over time for non-switching H_∞ controller (high γ). "Measured" represents the signal measured by the CGM sensor, "real" stands for the output of the system, while "reference" is for the output of the reference system W_{track}.

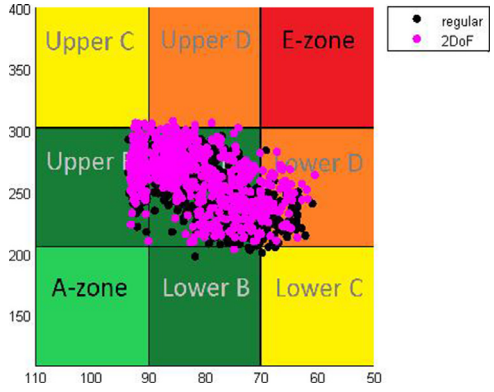

Fig. 18. Control variability grid analysis for switching controllers (low γ).

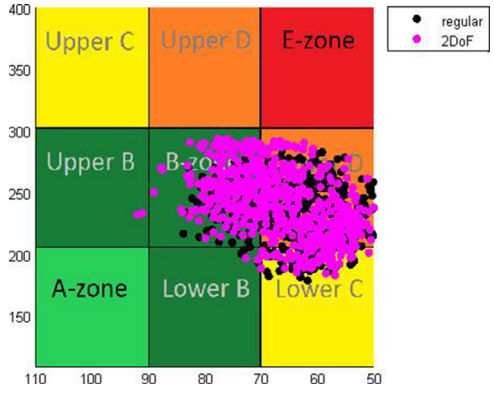

Fig. 19. Control variability grid analysis for switching controllers (high γ).

Table 3
Summary of meal intake simulation parameters.

Meal type	Chance of occurrence	Amount (g CHO)	Time
Breakfast	100%	50 – 90 g	6:00 – 10:00
Snack 1	50%	10 – 50 g	8:00 – 11:00
Lunch	100%	60 – 120 g	11:00 – 15:00
Snack 2	50%	10 – 30 g	15:00 – 18:00
Dinner	100%	35 – 95 g	18:00 – 22:00
Snack 3	50%	10 – 20 g	22:00 – 24:00

extending the controller with an integrator could be considered for robust methods as well.

Six virtual patients of the SimEdu in-silico simulator were used and 100 simulations were conducted for each patient with randomized initial states, parameter change, meal and physical activity profile. Uniform distribution was used in all cases. Table 3 summarizes the parameters of meal intakes. Physical activity occured 50% of the time starting between 9:00–12:00 and lasting for 1–4 hours. It can be seen from Table 3 that based on the relatively wide ranges of meal intake possibilities (simulating in this way the uncertain carbohydrate (CHO) estimation of the patients) even exterme meal intakes (400 g CHO) can occur. Moreover, by the uncertain time intervals the idea was to deal with the uncertain registration of the meal periods as well.

For all simulations a complete 48 hours simulation time interval was considered. The simulation results were evaluated based on the international standards of control variability grid analysis (CVGA) [33] and are presented below.

Figs. 14–17 shows the analysis for the switching and non-switching cases separating the case when only RP (low γ) or when

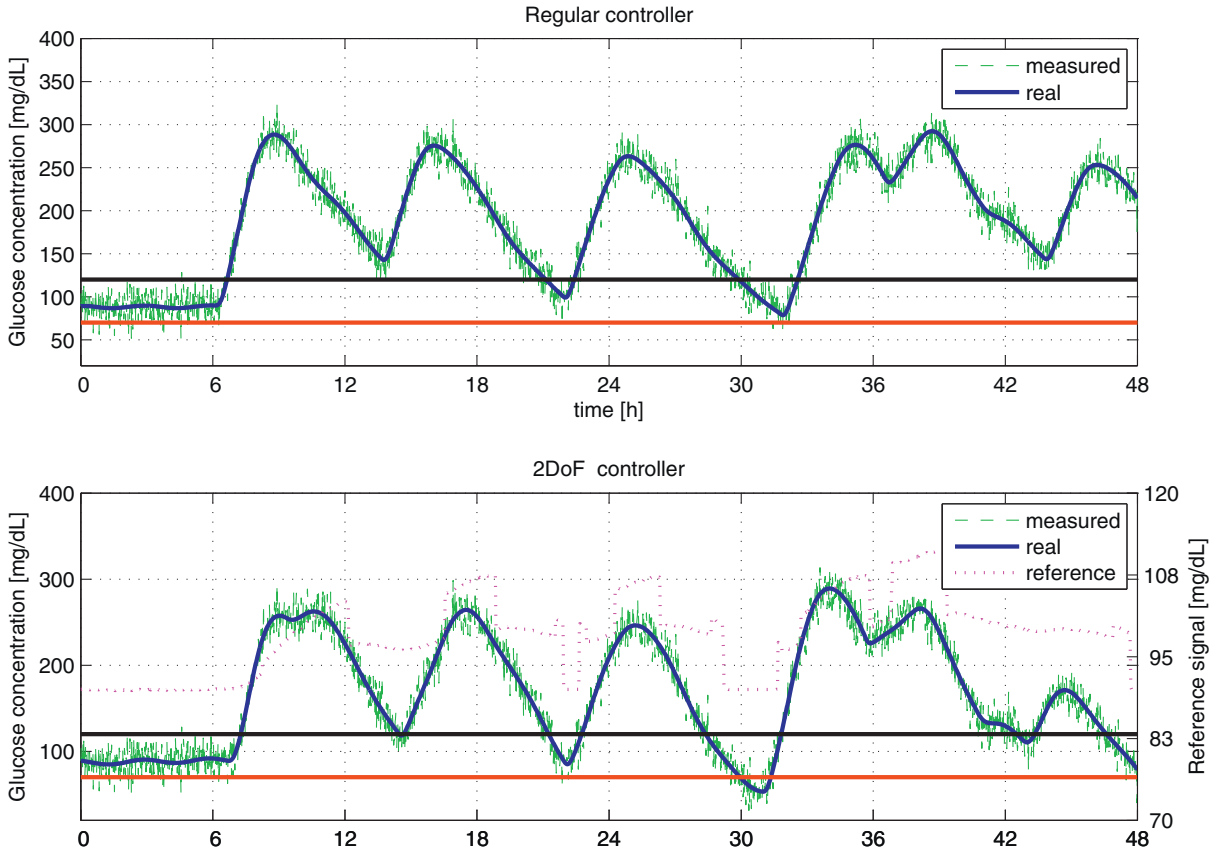

Fig. 20. Simulation over time for switching H_∞ controller (low γ). "Measured" represents the signal measured by the CGM sensor, "real" stands for the output of the system, while "reference" is for the output of the reference system W_{track}.

only RS (high γ) is satisfied. Instead of mmol/L the results are presented in the more widely used mg/dL format, for easier comparison.

Fig. 14 reflects the non-switching robust control results. It can be seen that taking the uncertain meal intake or time recording into account, for scenarios presented in Table 3 efficient and generally robust control cannot be achieved.

This result clearly presents the pros and cons of modern robust control methodology. Only guaranteeing RP does not mean that one could obtain a suitable controller. It is true that the controller achieved is generally applicable, but in a physiologically unacceptable range: big oscillations with big number of hypo- and hyperglycemic episodes that endanger diabetic patients' life.

This remark is true for focusing on RS as well (Fig. 15). Moreover, results in Fig. 15 demonstrate illustratively that RS is "below" in quality requirements than RP. Simulations over time are exemplified by Figs. 16 and 17 for both (RP and RS) cases.

In conclusion, it can be mentioned that for an individualized / personalized control (MPC or other methods used in the literature [13–19]) discussion is needed to adapt the problem on the given patient's characteristics, which however is not robust enough (it cannot handle Table 3 scenarios); hence, the two approaches should be combined. In other words, an adequate choice for the AP problem could be envisaged using a hierarchical control structure (not the scope of the current paper): individualized control solution adapted to the patient's physiology placed in a robust control framework to guarantee RP even for the worst cases.

By the switching control scheme (Fig. 18) the above mentioned remarks are true as well, but a qualitatively increased performance can be observed. RP is better matched with the physiological expectations due to the different working regimes where the controller is able to satisfy more adequately the physiological requirements. Results are still not the best, but due to the considered uncertain and extreme scenarios of Table 3 most of the hypoglycemic events (most dangerous for T1DM patients) can be avoided, while remaining ones are only moderate.

Regarding hyperglycemia, a considerable drop in CVGA from the results presented in Figs. 14 and 15 can be observed. Moreover, due to the high meal intake scenarios it is expected to have high glucose levels for T1DM patients. However, a hierarchical control structure mentioned above could better tune the results. Focusing only on RS (Fig. 19) the same remarks can be concluded as in the non-switching cases: although RS can be guaranteed, without satisfying the nominal performance requirements (in our case minimizing hypoglycemia) the control quality is worse.

In the switching cases, simulations over time are exemplified by Figs. 20 and 21 again for both (RP and RS) cases. In case of 2DOF control, the reference signal is also displayed.

Table 4 summarizes the simulation results for all the eight considered controller structures.

Analyzing these results, the following remarks can be made:

- The controllers achieved are not ideal ones, but they are able to prove their robust characteristics. With the extreme scenarios considered they guaranteed RP (or RS). In this way, a hierarchical control solution with individualized control adapted to the patient's physiology placed in a robust control framework to guarantee RP even in the worst cases can be a real alternative for the AP problem.
- For higher γ values, when only RS is met, blood glucose levels usually do not go as high when RP is satisfied. However, this comes at the cost of higher possibility for hypoglycemic episodes. 2DoF control can slightly shorten the duration of hy-

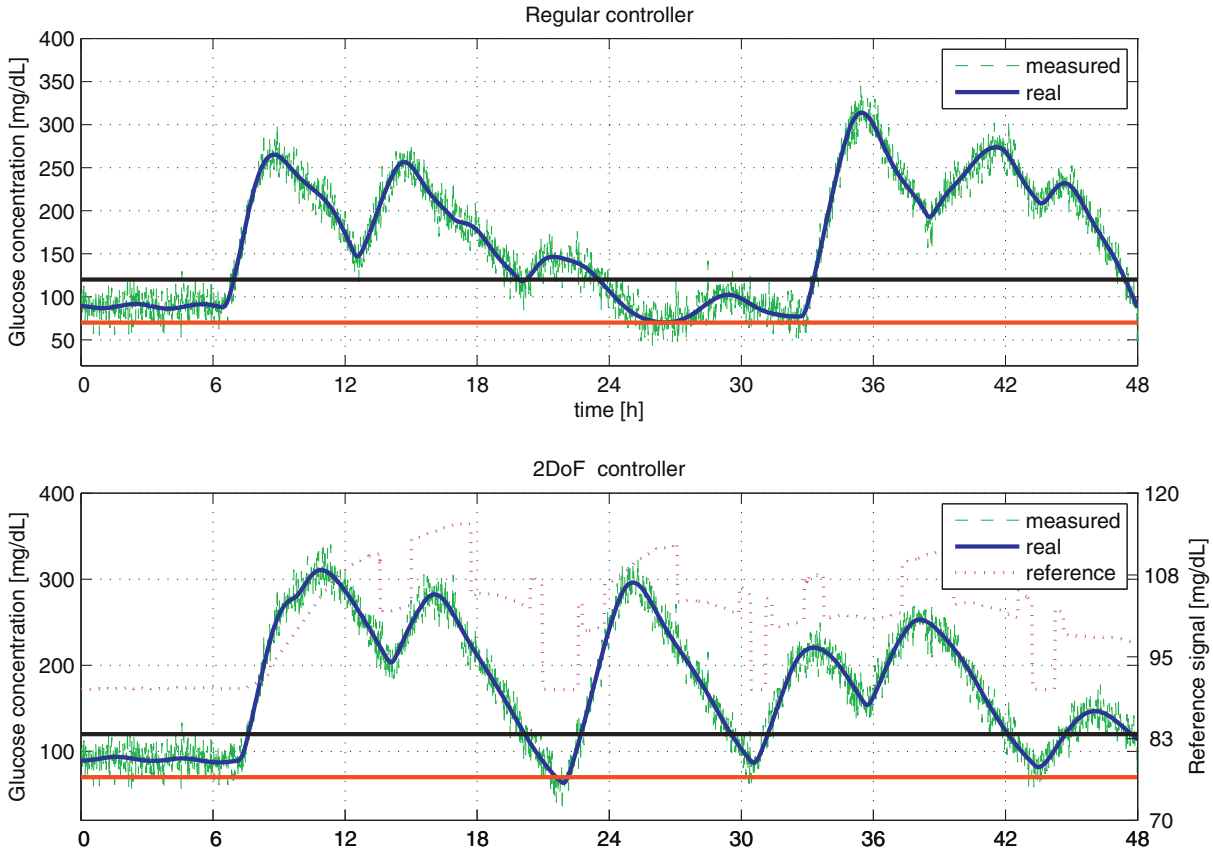

Fig. 21. Simulation over time for switching H_∞ controller (high γ). "Measured" represents the signal measured by the CGM sensor, "real" stands for the output of the system, while "reference" is for the output of the reference system W_{track}.

Table 4
Summary of simulation results for all controller types.

Controller	Hypo <4 mmol/L	Norm 4–6 mmol/L	Mild hyper 6–7.8 mmol/L	Hyper 6–11.1 mmol/L	Severe hyper >11.1 mmol/L
without switching					
Regular (low γ)	6.68%	25.98%	10.11%	26.67%	40.66%
Regular (high γ)	13.40%	28.34%	12.51%	30.03%	28.23%
2DoF (low γ)	3.13%	23.24%	9.01%	23.00%	50.63%
2DoF (high γ)	10.75%	26.93%	11.87%	30.42%	31.90%
with switching					
Regular (low γ)	5.35%	27.02%	8.14%	24.45%	43.17%
Regular (high γ)	11.39%	28.83%	9.13%	26.46%	33.33%
2DoF (low γ)	4.59%	25.49%	6.78%	21.28%	48.64%
2DoF (high γ)	10.41%	28.33%	8.32%	25.14%	36.13%

poglycemic episodes. It might be more favorable to provide disturbance estimation with a more capable tool, e.g.: Kalman filters or their extensions on sigma-point filtering [39, 42].

- Switching control could considerably improve the results by defining different working regimes where the controller could focus only on the given regimes' particularities. In this context we have designed the corresponding controller used in our robust control framework. Results were presented in [37] and Fig. 22 illustrates a simulation result of the system, where the shortcomings presented in the above roadmap were avoided.

5. Conclusions and further research directions

In this case study, the implementation of H_∞ controllers were investigated for the widely known and used T1DM model published in [10] and later updated in [25]. From the nonlinear model a nominal linear system was constructed with weighting functions representing the nonlinearity and parameter inaccuracies gained from expertise collected from real diabetic patient measurements or simulations of the validated SimEdu virtual simulator [25]. Using this configuration, regular, integral, 2DOF and integral 2DOF H_∞ robust controllers were implemented; both for switching and non-switching case. Simulations were conducted using 6 virtual patient data.

The study intended to show the possible issues appearing in H_∞ controller design for this particular artificial pancreas problem. The exact mathematical formulation of modern robust technique was combined with the empirical (knowledge-based) expertise gained from medical practice. The most practical issues have been addresses and results have been tested for extreme scenarios (high meal intakes and uncertain time recording). Switching control possibilities have been presented. Beside the robust control design roadmap given in the paper, the advantage of the research from control engineering point of view is to present the sensitivity of uncertainty weighting function selection, demonstrating that

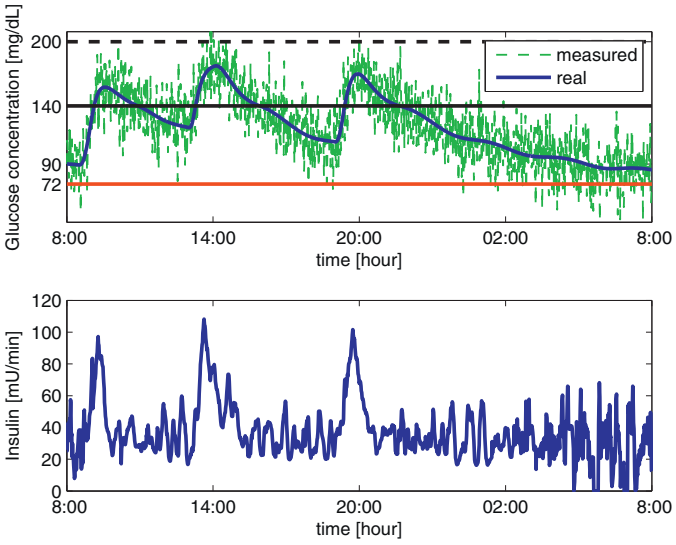

Fig. 22. Simulation over time for switching H_∞ controller (low γ). "Measured" represents the signal measured by the CGM sensor, "real" stands for the output of the system.

without given expertise (in this case medical knowledge) not only robust, but even unstable solution can be achieved. From clinical point of view the clear advantage is that once a robust controller is designed, there is no need to be redesigned on different patients or treatment scenarios; however, several medical data are needed increasing the knowledge required to achieve the robustness property.

Future research will focus on solving the H_∞ controller design on the investigated model using LPV modeling methodology, but also extended to a generalized LPV approach of Tensor Product model transformation [43–44]. Since the scheduling parameters cannot be measured directly, accurate estimation is needed and the resulting error must be considered and incorporated into the nominal model formulation [45–49]. Furthermore, H_2 and L_1 robust controllers can be implemented and compared with the ones presented in this paper. Hybrid controllers satisfying multiple constraints or hierarchical control structure combining individualized control strategies with modern robust methods are an option as well. Practical issues, such as sensor dynamics, errors and insulin pump failures should also be addressed together with other optimization methods e.g. [34–35, 42]. As a final remark it is important to mention that the aim of modern robust control is not to compete with individualized methodologies (like MPC), but to efficiently extend them giving extra safety guarantees.

Acknowledgment

This work was supported by the European Research Council (ERC) under the European Union's Horizon 2020 research and innovation program (grant agreement No 679681). The author is grateful for the Hungarian Artificial Pancreas Working Group centers for the real patient data provided.

Appendix A

The state-space representation of the T1DM model using the switching control and scheduling parameter combinations.

$$A_{1,1} = -k_{a,\mathrm{int}} - \delta_1 \Delta k_{a,\mathrm{int}}$$

$$A_{1,2} = \frac{k_{a,\mathrm{int}}}{V_G} + \delta_2 \frac{\Delta k_{a,\mathrm{int}}}{V_G}$$

$$A_{2,2} = -\frac{\rho_{4,\max}+\rho_{4,\min}}{2}\mu_1 - \frac{(\rho_{2,\max}+\rho_{2,\min})}{2} - \frac{R_{cl}}{2} - \delta_3 \frac{\rho_{4,\max}-\rho_{4,\min}}{2}\mu_1 - \delta_4 \frac{(\rho_{2,\max}-\rho_{2,\min})}{2} - \delta_5 \frac{R_{cl}}{2}$$

$$A_{2,3} = k_{12} + \delta_6 \Delta k_{12}$$

$$A_{2,4} = -\frac{(\rho_{1,\max}+\rho_{1,\min})}{2}(1-\mu_1) - \delta_7 \frac{(\rho_{1,\max}+\rho_{1,\min})}{2}(1-\mu_1)$$

$$A_{2,6} = -\mu_4 \frac{EGP_0 + \Delta EGP_0}{2} - \delta_8 \mu_4 \frac{EGP_0 + \Delta EGP_0}{2}$$

$$A_{3,2} = \frac{\rho_{4,\max}+\rho_{4,\min}}{2}\mu_2 + \delta_3 \frac{\rho_{4,\max}-\rho_{4,\min}}{2}\mu_2$$

$$A_{3,3} = -k_{12} - \delta_6 \Delta k_{12} - \frac{\rho_{5,\max}+\rho_{5,\min}}{2}\mu_3 - \delta_9 \frac{\rho_{5,\max}-\rho_{5,\min}}{2}\mu_3$$

$$A_{3,4} = \frac{(\rho_{1,\max}+\rho_{1,\min})}{2}(1-\mu_2) - \delta_7 \frac{(\rho_{1,\max}+\rho_{1,\min})}{2}(1-\mu_2)$$

$$A_{3,5} = -\frac{(\rho_{3,\max}+\rho_{3,\min})}{2}(1-\mu_3) - \delta_{10} \frac{(\rho_{3,\max}+\rho_{3,\min})}{2}(1-\mu_3)$$

$$A_{4,4} = -k_{b1} - \delta_{11} \Delta k_{b1}$$

$$A_{4,7} = S_{IT} k_{b1} + \delta_{12}(\Delta S_{IT} k_{b1} + S_{IT} \Delta k_{b1} + \Delta S_{IT} \Delta k_{b1})$$

$$A_{5,5} = -k_{b2} - \delta_{13} \Delta k_{b2}$$

$$A_{5,7} = S_{ID} k_{b2} + \delta_{14}(\Delta S_{ID} k_{b2} + S_{ID} \Delta k_{b2} + \Delta S_{ID} \Delta k_{b2})$$

$$A_{6,6} = -k_{b3} - \delta_{15} \Delta k_{b3}$$

$$A_{6,7} = S_{IE} k_{b3} + \delta_{16}(\Delta S_{IE} k_{b3} + S_{IE} \Delta k_{b3} + \Delta S_{IE} \Delta k_{b3})$$

$$A_{7,7} = -k_e - \delta_{17} \Delta k_e$$

$$A_{7,8} = \frac{k_a}{V_I} + \delta_{18} \frac{\Delta k_a}{V_I}$$

$$A_{8,8} = -k_a - \delta_{18} \Delta k_a$$

$$A_{8,9} = k_a + \delta_{18} \Delta k_a$$

$$A_{9,9} = A_{8,8}$$

$$B_{2,1} = B_{9,2} = C_{1,1} = 1, \mathit{otherwise}\ 0$$

References

[1] International Diabetes Federation, IDF Diabetes Atlas, 6th edn. Brussels, 2013.
[2] S. Wild, G. Roglic, A. Green, R. Sicree, H. King, Global prevalence of diabetes - estimates for the year 2000 and projections for 2030, Diabetes Care 27 (5) (2004) 1047–1053.
[3] J.E. Shaw, R.A. Sicree, P.Z. Zimmet, Global estimates of the prevalence of diabetes for 2010 and 2030, Diabetes Res. Clin. Pract. 87 (2010) 4–14.
[4] R. Harvey, Y. Wang, B. Grossman, M. Percival, W. Bevier, D. Finan, H. Zisser, D. Seborg, F. Jovanovic, F. Doyle, E. Dassau, Quest for the artificial pancreas, IEEE Eng. Med. Biol. Mag. 29 (2) (2010) 53–62.
[5] C. Cobelli, E. Renard, B. Kovatchev, Artificial Pancreas, Past, present and future, Diabetes 60 (11) (2011) 2672–2682.
[6] V.N. Shah, A. Shoskes, B. Tawfik, S.K. Garg, Closed-loop systems in the management of diabetes: past, present and future, Diabetes Technol. Ther. 16 (8) (2014) 477–490.
[7] F.J. Doyle, L.M. Huyett, J.B. Lee, H.C. Zisser, E. Dassau, Closed-loop artificial pancreas systems: engineering the algorithms, Diabetes Care 37 (2014) 1191–1197.
[8] F. Chee, F. Tyrone, Closed-loop control of blood glucose, Lecture Notes of Computer Science 368, Springer-Verlag, Berlin, 2007.
[9] R.N. Bergman, L.S. Philips, C. Cobelli, Physiologic evaluation of factors controlling glucose tolerance in man, J. Clin. Invest. 68 (1981) 1456–1467.
[10] R. Hovorka, V. Canonico, L.J. Chassin, U. Haueter, M. Massi-Benedetti, F.M Orsini, T.R. Pieber, H.C. Schaller, L. Schaupp, T. Vering, M.E. Wilinska, Nonlinear model predictive control of glucose concentration in subjects with type 1 diabetes, Physiol. Meas. 25 (2004) 905–920.
[11] J.T. Sorensen, A physiologic model of glucose metabolism in man and its use to design and assess improved insulin therapies for diabetes, Deptartment of Chemical Engineering. Massachusetts Institute of Technology PhD Thesis, 1985.
[12] L Magni, D.M. Raimondo, C.D. Man, G.D. Nicolao, B. Kovatchev, C. Cobelli, Model predictive control of glucose concentration in type 1 diabetic patients: an in silico trial, Biomed. Signal Process. Control (2009) 338–346.
[13] C.C. Palerm, Physiologic insulin delivery with insulin feedback: a control systems perspective, Comput. Methods Programs Biomed. 102 (2) (2011) 130–137.
[14] R. Hovorka, D. Elleri, H. Thabit, J.M. Allen, L. Leelarathna, R. El-Khairi, K. Kumareswaran, K. Caldwell, P. Calhoun, C. Kollman, H.R. Murphy, C.L. Acerini, M.E. Wilinska, M. Nodale, D.B. Dunger, Overnight closed-loop insulin delivery in young people with type 1 diabetes: a free-living, randomized clinical trial, Diabetes Care 37 (5) (2014) 1204–1211.

[15] B.P. Kovatchev, E. Renard, C. Cobelli, H.C. Zisser, P Keith-Hynes, S.M. Anderson, S.A. Brown, D.R. Chernavvsky, M.D. Breton, L.B. Mize, A. Farret, J. Place, D. Bruttomesso, S. Del Favero, F. Boscari, S. Galasso, A. Avogaro, L. Magni, F. Di Palma, C. Toffanin, M. Messori, E. Dassau, F.J. Doyle, Safety of outpatient closed-loop control: first randomized crossover trials of a wearable artificial pancreas, Diabetes Care 37 (7) (2014) 1789–1796.
[16] C. Ionescu, R. Hodrea, R. De Keyser, Impact of disturbance filter in nonlinear EPSAC predictive control of blood glucose level in type I diabetic patients, in: Proceedings of IEEE CCA, San Antonio, Texas USA, 2008, pp. 672–677.
[17] C. Ionescu, R. De Keyser, in: EPSAC predictive control of blood glucose level in type i diabetic patients, IEEE CDC-ECC, Sevilla, Spain, 2005, pp. 4845–4850.
[18] William Sansum Diabetes Center, Feasibility study using run-to-run control to optimize continuous glucose sensor bias, 2014.
[19] M. Phillip, T. Battelino, E. Atlas, O. Kordonouri, N. Bratina, S. Miller, T. Biester, M. Avebelj Stefania, I. Muller, S. Nimri, T.R. Danne, Nocturnal glucose control with an artificial pancreas at a diabetes camp, New England J. Med. 368 (2013) 824–833.
[20] K. Zhou, Robust and Optimal Control, Prentice Hall, New Jersey, 1996.
[21] C. Luni, J.E. Shoemaker, K.R. Sanft, L.R. Petzold, F.J. Doyle, Confidence from uncertainty - a multi-target drug screening method from robust control theory, BMC Syst. Bio. 4 (161) (2010) 1–10.
[22] R.S. Parker, F.J. Doyle III, J.H. Ward, N.A. Peppas, Robust H∞ glucose control in diabetes using a physiological model, AIChE J. 46 (12) (2000) 2537–2549.
[23] L. Kovács, B. Benyó, J. Bokor, Z. Benyó, Induced L2-norm minimization of glucose-insulin system for type I diabetic patients, Comput. Methods Programs Biomed. 102 (2) (2011) 105–118.
[24] P. Colmegna, R.S. Sanchez Pena, Analysis of three T1DM simulation models for evaluating robust closed-loop controllers, Comput. Methods Programs Biomed. 113 (3) (2014) 371–382.
[25] M. Wilinska, L. Chassin, C. Acerini, J. Allen, D. Dunger, R. Hovorka, Simulation environment to evaluate closed-loop insulin delivery systems in type 1 diabetes, J. Diabetes Sci. Technol. 4 (1) (2010) 132–144.
[26] A. Facchinetti, S.D. Favero, G. Sparacino, C. Cobelli, An online failure detection method of the glucose sensor-insulin pump system: improved overnight safety of type-1 diabetic subjects, IEEE Trans. Biomed. Eng. 60 (2) (2013) 406–416.
[27] A. Isidori, Nonlinear Control Systems, Springer-Verlag, London, 1995.
[28] L. Lee, Identification and Robust Control of Linear Parameter-Varying Systems, University of California at Berkeley, USA, 1997 Ph.D. thesis.
[29] L. Kovács, A. György, P. Szalay, B. Benyó, Z. Benyó, C. Hann, G.J. Chase, Investigating the applicability of LPV control theory to ICU models for glycaemic control, in: Proceedings of CONTROL UKACC Conference, Coventry, UK, 2010, pp. 577–582.
[30] A.P. White, G. Zhu, J. Choi, Linear Parameter-Varying Control For Engineering Applications, Springer-Verlag, London, 2013.
[31] L. Kovács, B. Kulcsár, A. György, Z. Benyó, Robust servo control of a novel type 1 diabetic model, Optimal Control Appl. Methods 32 (2011) 215–238.
[32] R. Gondhalekar, E. Dassau, H.C. Zisser, F.J. Doyle III, Periodic-zone model predictive control for diurnal closed-loop operation of an artificial pancreas, J. Diabetes Sci. Technol. 7 (2013) 1446–1460.
[33] L. Magni, D.M. Raimondo, C. Dalla Man, M. Breton, S. Patek, G. de Nicolao, C. Cobelli, B. Kovatchev, Evaluating the efficacy of closed-loop glucose regulation via control-variability grid analysis, J. Diabetes Sci. Technol. 2 (4) (2008) 630–635.
[34] M. Penet, H. Gueguen, A. Belmiloudi, A Robust receding horizon control approach to artificial glucose control for type 1 diabetes, in: Proceedings of IFAC Symposium on Nonliear Control Systems, Toulouse, France, 2013, pp. 833–838.
[35] P. Colmegna, R.S. Sanchez Pena, R. Gondhalekar, E. Dassau, F.J. Doyle III, Reducing glucose variability due to meals and postprandial exercise in T1DM using switched LPV control: In Silico studies., J. Diabetes Sci. Technol. 10 (3) (2016) 744–753.
[36] P. Colmegna, R.S. Sanchez Pena, R. Gondhalekar, E. Dassau, F.J. Doyle III, Reducing risks in type 1 diabetes using H∞ control, IEEE Trans. Biomed. Eng. 61 (12) (2014) 2939–2947.
[37] P. Szalay, Gy. Eigner, L. Kovács, Linear matrix inequality-based robust controller design for type-1 diabetes model, in: Proceedings of IFAC WC Conference, Cape Town, South Africa, 2014, pp. 9247–9252.
[38] B. Khan, G. Valencia-Palomo, J.A. Rossiter, C.N. Jones, R. Gondhalekar, Long horizon input parameterisations to enlarge the region of attraction of MPC, Optimal Control Appl. Methods 37 (1) (2016) 139–153.
[39] P. Szalay, Z. Benyo, L. Kovács, Long-term prediction for T1DM model during state-feedback control, in: Proceedings of 12th IEEE International Conference on Control & Automation (ICCA), Kathmandu, Nepal, 2016, pp. 311–316.
[40] L. Kovács, Zs. Almássy, E. Felszeghy, Gy. Kocsis, K. Wudi, E. Madarász, J. Fövényi, A. Körner, B. Benyó, Z. Benyó, L. Barkai, Quasi In-Silico simulation results of a robust blood glucose control algorithm, Diabetes Technology and Therapeutics (Abstracts of 4th International Conference on Advanced Technologies & Treatment for Diabetes, 13, 2011 242.
[41] L. Kovács, P. Szalay, P.I. Sas, Gy. Eigner, Zs. Almássy, E. Felszeghy, Gy. Kocsis, J. Fövényi, A. Körner, L. Kautzky, H. Soós, A. Orbán, T. Niederland, A. Juhászné Tuifel, T. Tóthné Sebestyén, A. Soós, A. Török, L. Barkai, Preliminary model-free results of a Hungarian robust artificial pancreas algorithm, Diabetes Technology and Therapeutics (Abstracts of 6th International Conference on Advanced Technologies & Treatment for Diabetes, 15, 2013 A-96.
[42] L. Kovács, P. Szalay, Uncertainties and modelling errors of type 1 diabetes models, in: H. Concentration, J.B. Kirschteiger, E. Jorgensen, L Renard, Re del (Eds.), Prediction Methods for Blood Glucose, (Ed.), Lecture Notes in Bioengineering, Springer, 2016, pp. 211–225.
[43] Gy. Eigner, J.K. Tar, I. Rudas, L. Kovács, LPV-based quality interpretations on modeling and control of diabetes, Acta Polytechnica Hungarica 13 (1) (2016) 171–190.
[44] R.E. Precup, C.A. Dragos, S. Preitl, M.B. Radac, E.M. Petriu, Novel tensor product models for automatic transmission system control, IEEE Syst. J. 6 (3) (2012) 488–498.
[45] U.R. Acharya, H. Fujita, M. Adama, O.S. Liha, V.K. Sudarshan, Automated characterization and classification of coronary artery disease and myocardial infarction by decomposition of ECG signals: a comparative study, Inf. Sci. 377 (2017) 17 29.
[46] N. Tomin, A. Zhukov, D. Sidorov, V. Kurbatsky, D. Panasetsky, V. Spiryaev, Random forest based model for preventing large-scale emergencies in power systems, Int. J. Artif. Intell. 13 (1) (2015) 211–228.
[47] H. Fujita, U.R. Acharya, V.K. Sudarshan, D.N. Ghista, S.V. Sree, W.J.E. Lim, J.E.W. Koh, Sudden cardiac death (SCD) prediction based on nonlinear heart rate variability features and SCD index, Appl. Soft Comput. 43 (2016) 510–519.
[48] O. Tursen, M. Tez, An application of Nelder–Mead heuristic-based hybrid algorithms: estimation of compartment model parameters, Int. J. Artif. Intell. 14 (1) (2016) 112–129.
[49] U.R. Acharya, V.K. Sudarshan, H. Fujita, D.N. Ghista, W.J.E. Lim, F. Molinari, M. Sankaranarayanan, Computer-aided diagnosis of diabetic subjects by heart rate variability signals using discrete wavelet transform method, Knowl.-Based Syst. 81 (2015) 56–64.